Marine Pollution Bulletin

Correlation of metals and degraded marine (micro)plastic litter in geologically similar coastal areas with different anthropogenic characteristics

--Manuscript Draft--

Manuscript Number:	MPB-D-22-00909
Article Type:	Research Paper
Keywords:	Degraded marine microplastic; Adsorbed metals; Adriatic Sea; Marine sediment
Corresponding Author:	Vlado Cuculić, Ph.D. Ruder Boskovic Institute: Institut Ruder Boskovic Zagreb, CROATIA
First Author:	Hana Fajković, PhD
Order of Authors:	Hana Fajković, PhD
	Neven Cukrov, PhD
	Stanislav Frančišković-Bilinski, PhD
	Laura Huljek
	Iva Kostanjšek
	Željko Kwokal
	Renata Matekalo
	Kristina Pikelj, PhD
	Vlado Cuculić, Ph.D.
Abstract:	The association and statistical correlation of anthropogenically important trace metals (TM) Cd, Cu, Pb, Zn with degraded marine microplastic (MP) in two marine systems, estuarine and coastal, in the Croatian Adriatic coastal area were assessed. The abundance of MP particles at both sites were primarily defined by local wave climate, due to which open coastal site had a 9-fold more microplastic particles (> 4 mm) compared to semi-closed estuarine, or twice as much considering bulk plastics. In general, higher metal adsorption was observed in the more anthropogenically influenced estuary (Mala Martinska) than in the open coastal site (Stupica Mala). The affinity of plastics for metals followed the order: polystyrene > polypropylene > low density polyethylene. Zinc showed the strongest affinity for all types of plastics at both sites, while the affinity of polystyrene for metals followed: Zn > Pb ≈ Cu > Cd.
Suggested Reviewers:	Hrissi Karapanagioti, PhD Professor, University of Patras Department of Chemistry karapanagioti@upatras.gr An outstanding expert in the field of marine microplastics research
	Véronique Lenoble, PhD Professor, University of Toulon veronique.lenoble@univ-tln.fr An expert in the research of trace metals and marine microplastics
	Hirofumi Hinata, PhD Professor, Ehime University hinata@cee.ehime-u.ac.jp Professor of Coastal engineering, an expert in marine microplastics research

Graphical Abstract

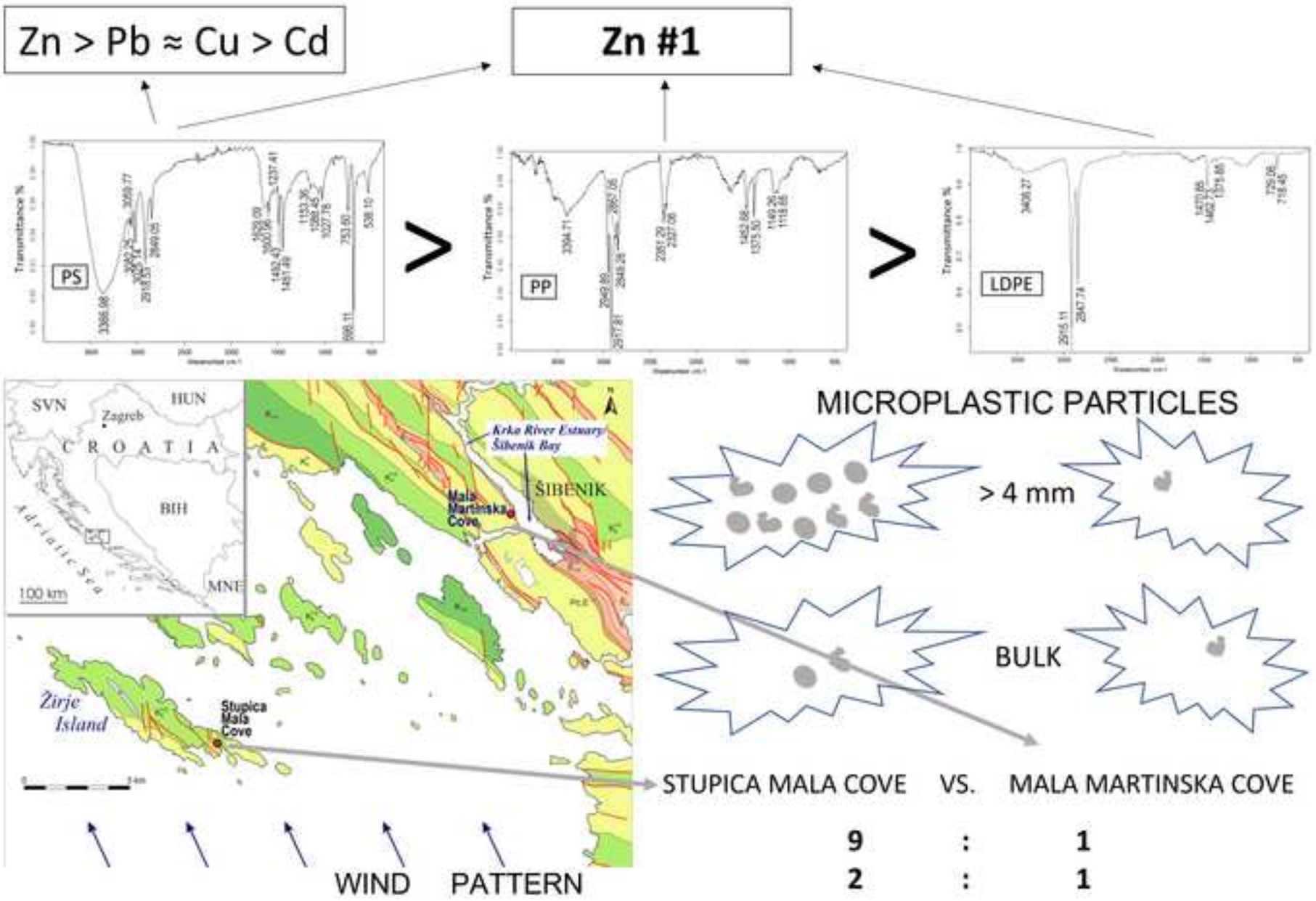

Highlights

- The abundance of microplastic particles is govern dominantly by local wind pattern
- Significantly higher metal adsorption in anthropogenically more affected site
- Adsorption affinity for toxic metals depends on the type of plastic and its size
- The affinity of plastics for metals follows the order: PS > PP > LDPE
- Zinc showed the strongest affinity for all plastic types

Correlation of metals and degraded marine (micro)plastic litter in geologically similar coastal areas with different anthropogenic characteristics

Hana Fajković[a], Neven Cukrov[b], Stanislav Frančišković-Bilinski[b], Laura Huljek[a], Iva Kostanjšek[a], Željko Kwokal[b], Renata Matekalo[a], Kristina Pikelj[a], Vlado Cuculić[b,*]

[a] University of Zagreb, Faculty of Science, Department of Geology, Horvatovac 102a, 10000 Zagreb, Croatia
[b] Ruđer Bošković Institute, Division for Marine and Environmental Research, Bijenička cesta 54, 10000 Zagreb, Croatia

*Corresponding author: cuculic@irb.hr

Abstract

The association and statistical correlation of anthropogenically important trace metals (TM) Cd, Cu, Pb, Zn with degraded marine microplastic (MP) in two marine systems, estuarine and coastal, in the Croatian Adriatic coastal area were assessed. The abundance of MP particles at both sites were primarily defined by local wave climate, due to which open coastal site had a 9-fold more microplastic particles (> 4 mm) compared to semi-closed estuarine, or twice as much considering bulk plastics. In general, higher metal adsorption was observed in the more anthropogenically influenced estuary (Mala Martinska) than in the open coastal site (Stupica Mala). The affinity of plastics for metals followed the order: polystyrene > polypropylene > low density polyethylene. Zinc showed the strongest affinity for all types of plastics at both sites, while the affinity of polystyrene for metals followed: Zn > Pb ≈ Cu > Cd.

Keywords: Degraded marine microplastic, Adsorbed metals, Adriatic Sea, Marine sediment

1. Introduction

Marine litter, with plastic litter as a dominant component, is a solid material that is abandoned in the marine and coastal environment. Plastic litter is widespread in oceans, and coastal areas all over the world and can be found even in the deepest ocean trenches (Bergmann et al., 2017; Hessler and Fildani, 2019; Kane and Fildani, 2021). Over time plastic items in the marine environment are degraded by physical processes (e.g. wave action), photolysis, and biodegradation (Andrady, 2011; Bonhomme et al., 2003; Kowalski et al., 2016) producing smaller particles called microplastics (MP). According to some authors, microplastics are particles smaller than 5 mm (Frias and Nash, 2019), and as such will be considered in this paper. In the last few decades, the distribution, fate, and impact of plastic litter in the marine environment have been subjected to many studies focused on beaches (Browne et al., 2011; Esiukova, 2017; Naji et al., 2017), sea surface (Cózar et al., 2014; Law et al., 2010), water column (Martin et al., 2017; Pedrotti et al., 2016; Peng et al., 2018), shallow sea bottom (Ioakeimidis et al., 2014; Lee et al., 2006; Martin et al., 2017; Mistri et al., 2017), and deeper bottom habitats (Bergmann et al., 2017; Courtene-Jones et al., 2017; Peng et al., 2018). Sagawa et al. (2018) compared amount of microplastics in bottom sediment, beach sediment and surface waters in coastal sea. An increasing number of publications reporting on plastics in marine environments indicates the emerging problem to be dealt with on the global level. Semi-enclosed seas with limited seawater exchange with the open ocean, such as the Mediterranean (Lacombe et al., 1981), are particularly prone to the increased input of plastic litter. The Mediterranean region with > 100 million coastal population, developed coastal tourism, and shipping routes has the potential to become one of the most impacted marine plastic accumulation zones (Cózar et al., 2015).

Due to its counterclockwise circulation causing transboundary effects, the semi-enclosed Adriatic Sea has been recognized as a preferential region for plastic accumulation within the Mediterranean region (Tziourrou et al., 2019), with particularly affected seabed (Pasquini et al., 2016). Over a decade ago Kwokal and Štefanović (2009, 2010) published the first assessment of marine plastic litter composition and sources in the Adriatic Sea, while more recently other authors recognized the Adriatic Sea as a significantly polluted marine area regarding plastic litter (Liubartseva et al., 2016; Mistri et al., 2017; Pasquini et al., 2016; Schmid et al., 2021; Vlachogianni et al., 2018; Zambianchi et al., 2017; Zeri et al., 2018). Marine plastic litter is multiple stressors in aquatic environments. One of the series of negative and for living world dangerous effects of floating plastic is the ability of these materials to adsorb various ecotoxicants, such as trace metals (TM) from the marine environment (Rochman, 2013). Elevated concentrations of certain TM (Cd, Pb, Cu, etc.) may be extremely toxic, harm biota and jeopardize the human food chain (Radix et al., 2000). Metal pollution especially occurs in rivers, estuaries, and coastal zones, due to the pronounced anthropogenic influence. The effects of metal pollution on the local environment and organisms can be long-lasting regardless of when the pollution began and stopped. Trace metals that are extremely toxic at natural and low concentrations are Cd and Pb. Because of their toxic characteristics at low concentrations, they were

recognized in local and international legislation, and according to the European Water Framework Directive (2008), they are considered priority pollutants. Copper and Zn are significant as micronutrients at low levels and exhibit toxic effects at higher concentrations. Studies of the interaction of TM and marine (micro)plastic particles are relatively new and started a decade ago (Ashton et al., 2010; Holmes et al., 2012; Nakashima et al., 2012; Rochman et al., 2014; Wang et al., 2017). Rochman et al. (2014) suggested that plastic debris accumulates larger amounts of metals the longer it remains in seawater. Also, they found a complex mixture of metals that are priority pollutants (Cd, Ni, Zn, and Pb) on plastic debris, while Munier and Bendell (2018) showed that amounts of metal on the polymers were similar to or greater than those in the bioavailable fraction in sediment. Massos and Turner (2017) measured Cd and Pb content in beached microplastics, while Lee et al. (2021) studied surface adsorption of metallic species onto microplastic in the natural marine environment. Ta and Babel (2020) investigated microplastic pollution with heavy metals in the aquaculture zone of the river estuary in Thailand. Moreover, model experiments have been made by Gao et al. (2021), where they studied trace metals with microplastic aging in various environmental media, while metal accumulation on aged microplastic in coastal waters compared between field and laboratory was obtained by Xie et al. (2021).

In the Adriatic Sea, Kwokal and Cuculić (2016) analyzed the distribution of mercury adsorbed on plastic pellets along the coast, while Maršić-Lučić et al. (2018) showed TM levels on microplastics in beach sediments from the Vis Island. More recently, Cuculić et al. (2021) and Fajković et al. (2021) described trace metals load on beached microplastics in the anthropogenically influenced estuary and the correlated microplastic type and metal association.

In this study, we examined the interaction of potentially (eco)toxic metals with beached microplastics collected at two locations in the Croatian Adriatic coastal area, which have similar geochemical and sedimentological characteristics, but different anthropogenic influences. For the first time, the composition of the plastic particles was identified and correlated with the trace metals in the Adriatic Sea. Statistical analysis was performed to evaluate the association of TMs with microplastic material in two different environments. Furthermore, sediment and seawater samples were also analyzed to obtain comprehensive environmental information on the studied depositional environments and to determine exchangeable phases in sediment.

2. Materials and Methods

2.1. Study area

The study area is set on two coves at the central part of the Croatian Adriatic Sea, Stupica Mala (SM) and Mala Martinska (MM) (Figure 1). Stupica Mala (SM) is situated in the south-eastern part of the Žirje Island, the most remote inhabited island of the Šibenik archipelago. Žirje Island's surface area is 15.43 km^2, it is 12 km long, and its average width is 1.2 km (CHI, 2015). This location was selected for research due to its remote position from the mainland coast and consequently low anthropogenic influence.

However, although uninhabited, SM is one of the preferred locations for nautical tourists. Furthermore, due to the outer position of the whole island and the south-eastward orientation of the SM cove, it is easily reachable for the floating marine litter carried by the waves of the dominant southeast wind (*Jugo/Scirocco*) from the open sea (Poulain and Cushman-Roisin, 2001). Unlike the SM site, Mala Martinska cove (MM) is situated in the Šibenik Bay, the sheltered part of the Krka River estuary. The MM cove is facing the populated city of Šibenik, known for its developed tourism, marine traffic, aquaculture, shipbuilding industry, and former manganese ferroalloy plant. Both study locations are microtidal areas (tidal range up to 0.5 m). Chosen locations are situated along the carbonate coast, typical for most of the Croatian mainland and islands (Pikelj and Juračić, 2013). Cretaceous carbonates dominate around the SM and the whole Žirje Island area, while Eocene carbonates occur to a lesser extent within the Šibenik Bay and near the MM study location as well (Figure 1). More erodible Eocene flysch reaches the sea only in the limited area of the SE part of the Šibenik Bay (Figure 1). In line with the prevailing carbonate bedrock, terrigenous sediment input is low, and marine coastal sediment is expected to be mostly of carbonate biogenous origin as in the case of similar coastal environments (Pikelj, 2010; Prohić et al., 1989; Puhr and Pikelj, 2012).

2.2. Sampling and sample preparation

Beached bulk sample material i.e., debris, seawater, and sediment were collected in August 2019 on the cove at MM (Šibenik Bay) and in July 2020 on the cove at SM (Žirje Island). Sampled debris material consisted of wooden particles, seagrass wrack, and marine plastic litter. SM and MM bulk debris samples were manually collected and separated into fractions by size (> 4 mm, 2 – 4 mm, 1 – 2 mm, 0.250 – 1 mm) by sieving. From fractions > 1 mm plastic particles were singled out with tweezers and a needle, while from smaller fractions ZEISS® loupe with a magnification level of 3.2x was used.

Seawater for trace metal analysis was collected simultaneously with the debris and the sediment sampling at both locations. Seawater samples for TM determination were collected in pre-cleaned perfluoroalkoxy (PFA) bottles (0.25 L, NALGENE®) using a clean sampling technique (Horowitz, 1997), to prevent loss of material, due to TM adsorption on the bottle's walls. Immediately upon sampling, half the volume of each sample was filtered through 0.45 µm cellulose nitrate membrane filters (Sartorius, Göttingen, Germany) and all samples (filtered and unfiltered) were acidified with concentrated Suprapur® nitric acid (Merck) to pH ~ 2. Due to the voltammetric technique demands, all samples were UV irradiated (24 h) before the TM measurements to secure detection of the total metal (unfiltered samples) and total dissolved metal (filtered samples).

The uppermost five cm of surface sediment was sampled at both locations: at the MM location sediment was collected from the lower intertidal zone, while from the SM location samples were collected in the upper intertidal (SM-A), lower intertidal (SM-B), and subtidal zone (SM-C). All sediment samples were air-dried and gently mixed until homogenized. Representative subsamples from each sediment sample were separated and powdered for further analyses.

2.3. Analyses

2.3.1 Analysis performed on plastic particles

After hand separation of plastic particles from bulk debris material, particles were analyzed with Fourier Transform Infrared Spectroscopy (FTIR) on the Tensor 27 device, and aliquots were separated and additionally used for the analysis of adsorbed TM on the surface of plastic particles. The FTIR spectrum was recorded in the region of 400 - 4000 cm^{-1}, with the attenuated total reflectance (ATR). In total 96 particles were isolated. All plastic particles from the SM study site were extracted from a fraction > 4 mm, counting in total 71 particles. The total number of analyzed particles from the MM study site was 25 and they were extracted from pre-sieved fractions.

For the TM analysis, dry plastics samples were weighed in pre-cleaned quartz tubes and the mixture of 5 mL ultra-clean acids (3 ml HNO_3, 2 mL $HClO_4$) was added prior to 24 h stirring. Analysis was performed on 23 samples of plastic particles, 15 from SM (all > 4 mm) and 8 from MM. The polymer type was formerly predefined for particles > 4 mm, while polystyrene from MM was separated due to its typical appearance. The fractionated bulk material from MM was used as such, without determining the polymer type. Digests with leached metals were quantitatively pipetted to 100 mL volumetric flasks and diluted to mark with Milli-Q® water. Digested solutions were transferred into clean PFA bottles (0.25 L), and prior to analysis UV irradiated for 24 h to decompose organic complexes that stabilize TM in solution. Concentrations of TM leached from samples were determined by Metrohm Autolab modular potentiostat/galvanostat Autolab PGSTAT204, connected with a three-electrode system Metrohm 663 VA STAND (Utrecht, The Netherlands). The working electrode used was a static mercury drop electrode (SMDE), while the reference electrode was Ag/AgCl glass electrode. The used electrochemical method (Bard and Faulkner, 2001, Cuculić et al., 2009) was differential pulse anodic stripping voltammetry (DPASV). Limit of quantification, LOQ, obtained in acidic Milli-Q® water (Merck) were 1, 2, 5, and 10 ng L^{-1} for Cd, Pb, Cu, and Zn in water samples, respectively, based on a standard addition method and 10σ rule (for 10 min accumulation time). Measurement uncertainty was calculated as 95% confidence interval, (c.i.).

2.3.2. Analysis of trace metals in seawater

Concentrations of total metal (unfiltered) and total dissolved metal (filtered) in seawater samples (15 mL) were determined by the DPASV method, previously described in section 2.3.1. The quality control of the applied method for trace metals analysis in seawater was checked by measuring the standard reference material (SRM) for trace metals in ocean seawater (NASS-6, National Research Council of Canada), with certified values (µg/L): Cd 0.0311±0.0019, Pb 0.006±0.002, Cu 0.248±0.025 and Zn 0.257±0.02. All determined concentrations were measured in triplicate and were found to be within 5 % of certified values.

2.3.3. Analysis performed on sediment

In the sediment, the grain size distribution, the amount of carbonate component, X-ray phase analysis, total organic carbon and exchangeable fraction by BCR analysis were determined.

For grain size analysis approximately 200 g of dried sediment were weighed, stirred with distilled water, and wet sieved through 7 standard 20 cm Θ stainless steel sieves. Mud fractions (< 0.063 mm) were collected in suspension and analyzed using Micromeritics SediGraph 5100 following standard sedigraph procedures (MICROMERITICS, 2002) (detailed grain size analysis description is given in Puhr and Pikelj (2012)). Granulometric parameters were calculated according to the Folk and Ward method (Folk and Ward, 1957), while sediments were classified according to Folk (1954).

The carbonate content in the sediment was determined according to the standard method EN ISO 10693 (2014) using the Scheibler apparatus. The carbonate content was determined on the pulverized bulk samples of the pulverized fractions (1 – 2 mm, 0.5 – 1 mm, 0.25 – 0.5 mm, 0.125 – 0.25 mm, 0.063 – 0.125 mm, < 0.063 mm) of all samples. Gravel fraction found in samples contained only recognizable carbonate rock fragments and it was excluded from this analysis. The mass of each analyzed subsample was ~ 300 mg.

Qualitative and semiquantitative X-ray powder diffraction analysis (XRPD), i.e. phase analysis was carried out on bulk sediment and mud fraction (< 0.063 mm) SM-B and MM samples. SM-B sample was chosen as an analog sample to MM and the transitional sample between SM-A and SM-C samples. Sediment samples were powdered in an agate mortar and pressed into an aluminum holder. The mineral composition was determined using a Philips X'pert powder diffractometer with CuKα radiation from the tube at 40 kV and 45 mA, collecting an X-ray diffraction dataset from 4° to 63° 2Θ. Diffraction patterns were compared with Joint Committee on Powder Diffraction Standards (JCPDS) database.

Total organic carbon (TOC) was analyzed in dried and homogenized sediment samples SM-B and MM (~ 20 mg), which were acidified with 2M HCl and left overnight at a temperature of less than 40 °C to remove inorganic carbon from the sample. The sample was burned at a temperature of 900 °C, using a combined catalyst (Pt/Si CoC), in a high temperature oxidation chamber in a stream of extra clean air and oxygen, and the resulting CO_2 is determined using a non-dispersive infrared detector (NDIR). Samples were measured in a solid sample module SSM-5000A connected to a TOC-VCPH organic carbon analyzer (Shimadzu, Japan). Measurements were made in triplicates, and the mean values were given. The quantification limit for this method was 0.035 %.

The exchangeable fraction of metals from the mud fraction of samples SM-B and MM was analyzed by the first step of the three-step BCR sequential analysis with additional *aqua regia (AR*) step, as described in Rauret et al. (1999) and Pueyo et al. (2008). The analysis for each sample was performed in duplicates. Exchangeable fraction represents elements

weakly adsorbed on the surface of solid i.e. minerals by relatively weak electrostatic interactions as well as elements that can be released by ion-exchange processes (Filgueiras et al. 2002), and are described as bioavailable elements that can be easily taken by plants end enter the food chain (Fernández Alborés et al., 2000; Hernández-Moreno et al., 1999). Multielement analysis of the prepared samples was performed by High Resolution Inductively Coupled Plasma Mass Spectrometry (HR-ICP-MS) using an Element 2 instrument (Thermo, Bremen, Germany). The typical instrument conditions and measurement parameters used throughout the work are reported in Fiket et al. (2017). The additional *AR* analysis was preformed and gave an insight into a (semi)total composition of the sediments, which can be found in detail in Huljek et al. (2021). The mass of the samples used for the analysis was ~500 mg with the adjusted volumes.

2.3.4 Statistical analyses

Software Statistica 6.0 (StatSoft, 2001) was used for the following statistical analyses performed within this study:

a) Determination of basic statistical parameters, and correlation by calculating Pearson's correlation coefficient. It is presented in the form of a correlation matrix to determine the strength of the linear correlation of mass fractions between studied elements. Obtained values were statistically significant at $p < 0.05$.
b) Boxplot method was used to determine anomalies of TM on plastic particles. Anomalies are divided into outliers (weaker anomalies) and extremes (larger anomalies). Normal or lognormal box-plots are constructed based on the empirical cumulative distribution plots. The box length was in the interquartile range, where outlier values were defined between 1.5 and 3 box lengths from the upper or lower edge of the box. Extremes are values more than 3 box lengths from the edge of the box (Kaufman and Rousseeuw, 1990; Reimann et al., 2005).
c) Cluster analysis of R-mode presents linkages between variables (in our case trace metals) and is usually presented in the form of a dendrogram.

More details about all used statistical analyses can be found in Davis (2002) and Halamić et al. (2001).

3. Results

3.1. *Plastic particles analysis and assessment of metals on plastics and seawater*

Plastic type determination of isolated particles was performed on an FTIR-ATR in the region of 400-4000 cm^{-1}. All data were collected using Bruker software OPUS (Bruker Optics GmbH), and identification was additionally substantiated by literature (Jung et al., 2018). Results of FTIR-ATR analysis and the amount of isolated microplastic particles in all subsamples are presented in Table 1. A total of 71 plastic particles (fraction > 4 mm) from SM were classified into 4 groups: low density polyethylene (67.6 %), polypropylene (21 %), and polystyrene (2.8 %). Obtained spectra of 8.5 % of samples did not match with spectra of any type of plastic either in the database or in the literature and are defined as not determined (n.d.). A total of 25 plastic particles separated from MM (all fractions) were

classified into 5 groups: polystyrenes (40 %), polypropylene (36 %), high-density polyethylene (8 %), and low-density polyethylene (8 %), while the determination of polymer type was not obtained for 8 % of samples. Representative FTIR spectra of defined plastic type are presented in Figure 2.

Trace metal mass fractions were measured (mg of metal / kg of the sample) on 15 SM (Table 2) and 8 MM samples (Table 3). Prior to analysis of mass fraction of adsorbed metals on the surface, plastic type was defined for particles from SM, while from MM analysis were performed on a bulk plastic material of each fraction, and additionally on polystyrene particles (PS).

The concentrations of TM measured in the seawater samples collected at MM and SM are presented in Table 4. All measurements were performed in filtered (dissolved metal) and unfiltered (total metal) seawater samples. All metal concentrations were characteristic of slightly anthropogenically influenced areas of the Adriatic Sea, and in the range previously described by Cuculić et al. (2009).

3.2. Analysis performed on sediment

All analyzed sediment samples were classified as sandy gravels (sG) (Figure 3). Sand and gravel fractions varied between 27 and 70 % in all samples, while the mud fraction was scarce. Sediment medians ranged between 1.76 mm (SM-C) and 6.13 mm (SM-A), while their mean showed a smaller range, between 1.47 mm (SM-C) and 2.43 mm (MM). The highest similarity was observed between samples MM and SM-B regarding fractions percentage and mean grain size (Figure 3).

The carbonate component was rather high in all bulk samples, ranging between 86.2 and 97.6 %. In all analyzed sediment fractions carbonate was decreasing from ~ 99 % in coarse sand fractions to ~ 50 % in mud fractions (Table 5).

Qualitative and semiquantitative XRPD analysis showed that the main minerals in the SM-B samples were carbonates: calcite as the main mineral with aragonite and Mg-calcite as less represented carbonates. Quartz is less represented in the SM-B sample. Calcite also dominates the MM sediment sample, while aragonite and quartz are less represented, and quartz was detected only in the mud fraction (Table 6). Halite in all samples is the residue after sediment drying.

The total organic carbon (TOC) in surface sediment was found to be 1.07 % at SM-B and 6.2 % at MM, respectively. Results of a chemical analysis performed on the sediments are presented in Table 7. The first step of the three-step BCR sequential analysis for both samples shows relatively low values of Pb, Cd and Cu. These do not exceed 2 mg/kg, and Cu was below the limit of detection in 25 % of the samples. Zinc has a wide range of concentrations, from 0.811 mg/kg in the SM sample to 56.34 mg/kg in the MM sample, respectively. These values in the exchangeable fraction, which is provided by BCR step one, do not exceed any of the threshold limit values in different legislation (AGI, 2019; EUR-Lex - 32000L0060 – EN, EUR-Lex - 32010L0075 – EN, Bakke et al., 2010). In addition, control AR analysis carried out in Huljek et al. (2021) provided an insight into the

overall chemical composition of the samples, where the contents of the main elements (Ca, Mg, Na, etc.) confirm that the main phase component is calcite, as determined in qualitative XRPD analysis. This high Ca concentrations are also confirmed with carbonate content analysis.

3.3. Results of statistical analyses

Basic statistical parameters (Valid N, Mean, Median, Minimum, Maximum, Range, Variance, and Standard Deviation) were calculated separately for each of the two studied locations (SM and MM) and are presented in Table 8.

Correlation matrices were calculated separately for each studied location (SM and MM) and are presented in Table 9 for SM and MM locations. The correlation matrix should reveal mutual correlations between heavy metals adsorbed on plastic particles, separately for both locations. Statistically, significant correlations are marked in bold.

Boxplot diagrams were constructed for all studied elements determined on collected plastic samples, using a complete dataset including both studied locations, with the aim to determine their statistical anomalies (extremes and outliers) (Figure 4). At the SM location all studied elements show anomalies, mostly extremes. Zinc at SM has only one anomaly (extreme) in sample PS_a. Cadmium at SM has two anomalies: extreme in sample LDPE_b and outlier in PP_b. Lead at SM has only one anomaly (extreme) in sample PP_a. Copper at SM has three anomalies: extremes in samples PP_d and in PS_a, and outlier in sample LDPE_d. At MM location Zn, Pb, and Cu don't show any statistical anomaly, while Cd shows one positive and one negative outlier: Sample PS; 0.250 – 1 mm has positive Cd outlier, while sample Bulk; 2 – 4 mm has negative Cd outlier, meaning that this sample has a very low concentration of Cd.

R-mode cluster analysis was performed separately for each location to investigate linkages between studied metals adsorbed on plastic particles elements (Figure 5). At SM R-mode cluster analysis shows the linkage between Cu and Cd, to which is then linked Zn and Pb is then linked to them as a separate branch of dendrogram. At MM R-mode cluster analysis shows a close linkage between Cu and Pb. Then Cd is related to them, followed by Zn, which forms a separate branch of the dendrogram.

4. Discussion

To determine the TM load on isolated plastic particles, samples from two coastal coves of different anthropogenic influences were compared.

FTIR-ATR analysis of the plastic type showed that debris from SM consisted of more diverse plastic particles than the samples from the MM site (Table 1). At the SM site, LDPE was the predominant plastic type for fraction > 4 mm (67.6 %), followed by PP (21 %), while at the MM site PS and PP were almost evenly distributed, 40 % and 36 %, respectively. An abundance of MP also varies from site to site, with the number at site SM predominating. When comparing the particles > 4 mm, the number of MP at SM site was almost 9-fold higher than at MM site. Considering the total amount of all fractions from MM site ($\sum$ = 1.12 MP/g debris) and comparing it with the number of MP particles > 4 mm from the SM site, the number decreases, but is still twice as high. This distribution is due to the local wave climate (Poulain and Cushman-Roisin, 2001) and the fact that SM cove is completely exposed to the waves caused by the southeast wind (*Jugo/Scirocco*).

For valid analysis of TM associated with the plastic particles and to evade possible sample contamination, particles were divided into aliquots, and such sample management was possible only on a large particle, i.e., > 4 mm. Therefore, only SM particles > 4 mm were analyzed for TM load. Due to the homogeneity of isolated particles at the MM location analysis of three additional fractions was conducted (2 – 4 mm, 1 – 2 mm, 0.250 – 1 mm), on isolated particles as a bulk material defined by visual similarity, and on polystyrene particles, due to their typical and unambiguous appearance.

Analysis of TM at the SM site (Table 2) enabled a good insight into the adsorption of a specific element on a plastic type. Results suggested a strong affinity of PE for zinc, PP for lead, and an overall greater affinity of PS for all measured TM. However, analysis at the MM site (Table 3) showed the significant connection of metal load and MP size fraction and it was more pronounced at PS plastic type. These findings are consistent with a previous model study where Barus et al. (2021) have shown that PS has a large capacity for adsorption of TM in aquatic systems. Moreover, Graca et al. (2014) described styrofoam debris in the southern Baltic coastal area as a carrier within an ecosystem. The bulk plastic material had almost 6-fold higher affinity for a Zn and Pb in fraction 0.250 – 1 mm compared to > 4 mm and 4-time higher for Cu for the same fractions. The distinction among fractions was visible within the PS, as well, however with a lesser difference. Zinc, Pb, and Cd approximately doubled affinity for PS 0.250 – 1 mm compared to PS > 4 mm, while Cu followed with the 1.5-fold higher value for PS. Similarly, Hildebrandt et al. (2021) found in a model experiment that smaller microplastics showed a significantly higher sorption capacity compared to larger particles. In our study, only Cd showed an exception from the observed increase of a mass fraction on the surface of the smallest particle fraction in bulk material, where even a slight decrease was determined when comparing the fraction 0.250 – 1 mm with the fraction > 4 mm.

When the metal mass fraction of all plastic particles from the SM site is presented as an arithmetic mean value (Table 2), which could be considered as an analysis of bulk > 4

mm, the value of the mean mass fraction for Zn is 8 mg/kg and is the most abundant element with similar values at both sites. However, when the arithmetic values are calculated without the particle PS_a, which is an outlier for Zn, the value significantly decreases (3.4 mg/kg). When comparing the sites by particles > 4 mm, higher metal amounts on MP particles at the SM location were detected for Cd and Pb, while at the MM location Zn and Cu were the highest. On the other hand, concentrations of Zn and Cd were higher in seawater samples at SM, while Pb and Cu had higher values at MM. Such results are an indication that the processes in nature cannot be interpreted unanimously. As indicated by Munier and Bendell (2018) the amounts of metals extracted from the analyzed plastic particles are higher than the values obtained from the exchangeable (bioavailable) fraction of the sediment. That can be seen at the SM location, where some elements (Pd and Cu) were below the detection limit in BCR1, while they were measurable at plastic particles, 6.3 mg/kg and 1.5 mg/kg for Pb and Cu, respectively.

Basic statistical parameters of leached TM from plastic showed that of the four studied elements three of them show higher mean concentrations at location MM (Table 8). Among them, Zn shows more than 5 times higher mean concentrations at MM. This could be explained by the fact that it is in the rather enclosed bay within the Krka River estuary, just opposite Šibenik town, which could be the source of sewage and other pollution. Lead more than doubled its mean concentration at the MM site compared to the SM site. It can be assumed it was due to a much stronger anthropogenic influence at the MM site, caused by the vicinity of the Šibenik port. Moreover, Cu mean concentration was approximately 6 times higher at MM than at the SM site. However, Cd was the only element behaving differently and its mean concentration doubled at SM compared to MM. This could suggest that Šibenik Bay was not a source of elevated cadmium levels. Increased Cd concentrations at the SM site could be due to the typical seawater habitat, while at MM there is a strong influence of freshwater (brackish water, salinity = 6). It is well known from the literature that Cd concentrations are naturally higher in seawater since dissolved Cd has a high affinity to bind chlorides (Neff, 2002). Moreover, elevated Cd concentrations could be the result of antifouling paints, since SM cove is a natural harbour hosting a significant number of recreational vessels. Sample LDPE_9 at the SM site had an extremely high amount of Cd (2.83 µg/g). This anomalous sample significantly contributes to the high mean Cd value at this location. Therefore, recalculation of the Cd means from SM by excluding the extremely anomalous mass fraction gives a mean value of 0.25. This is significantly lower compared to the mean concentration calculated for all samples, but still, it is higher compared to Cd mean mass fraction at the MM site. The median is less sensitive to extreme values than the arithmetic means and therefore it is more suitable for irregular asymmetric distributions like our dataset for Cd. For other metals, the median is also much higher at anthropogenically influenced location MM. Moreover, the median value for Cd is only slightly higher at MM than at SM (0.17 vs. 0.14). Hence, we can assume that except for some very anomalous plastic particles, average concentrations of Cd were similar at both locations and slightly elevated at the SM site. On the contrary, at the MM location Zn, Pb, and Cu did not show any statistical anomaly, while Cd revealed one positive and one negative outlier (anomaly of lower degree) on the boxplot diagram

(Figure 4): Sample PS; 0.250 – 1 mm had positive Cd outlier, while sample Bulk; 2 – 4 mm demonstrated negative Cd outlier, indicating that Cd amount was significantly low in this sample. The anthropogenic impact of the city of Šibenik is obvious at the MM site, and the concentrations of most elements are significantly higher than at the SM location. Therefore, there were almost no anomalies because the concentrations of the elements showed a uniform distribution. However, at the SM location, all studied elements showed anomalies, mostly extremes (Figure 4). Zinc at SM had only one anomaly (extreme) in sample PS_a. Cadmium at SM has two anomalies: extreme in sample LDPE_b and outlier in PP_b. Lead at SM has only one anomaly (extreme) in sample PP_a. Copper at SM has three anomalies: extremes in samples PP_d and PS_a, and outliers in sample LDPE_d. This was due to a rather unpolluted location (SM), under the prevailing influence of the open sea, where a majority of samples showed relatively low concentrations. However, some studied particles could be anthropogenically influenced, due to tourist season.

At MM R-mode cluster analysis showed the close linkage between Cu and Pb, while Cd was related to them, followed by Zn, which formed a separate branch of the dendrogram. At SM R-mode cluster analysis showed the linkage between Cu and Cd, to which Zn and Pb were linked as a separate branch of the dendogram.

The results of the grain size analysis revealed that all SM sediment samples are sandy gravels (Figure 3). Gravel fraction prevails in the intertidal samples SM-A and SM–B, while in the marine sample SM-C gravel and sand share are approximately equally represented. Such grain size distribution showed a seaward decreasing trend of gravel fraction. Share of sand and mud fraction follows the opposite trend, while mud fraction is generally low: < 5 % in all sediments. Accordingly, mean grain size is decreasing in the seaward direction, samples SM-A and SM-B are moderately sorted, while sample SM-C is poorly sorted. In general, the coarseness of these intertidal and shallow marine sediments is the partial result of the coast formed mostly in carbonate bedrock, lacking terrigenous sediment input (Pikelj, 2010). Therefore, high carbonate content (94 – 97 %) in all SM sediments is expected (Table 5). Calcite is the main mineral phase originating partially from rock fragments, while aragonite, Mg-calcite, and part of calcite are of biogenous origin (marine invertebrate shell debris; Table 6). Such mineral composition is typical for the nearshore and marine sediments of the eastern Adriatic coast (Pikelj, 2010, Pikelj et al., 2016). The share of carbonates is decreasing seaward, in line with the decreasing mean grain size, indicating that quartz is present in fine-grained fractions. Furthermore, the coarseness of the SM sediment is partially a result of the exposure to waves generated by the dominant SE wind (*Jugo/Scirocco*). Adriatic coarse-grained sediment of predominant carbonate mineral composition (with small quantities of admixed quartz) does not act as a contaminant collector due to the low specific surface area (Vdović and Juračić, 1993). For the same reason, TOC in the SM-B sample is low (1.07 %).

Intertidal MM sediment is classified as poorly sorted sandy gravel, showing similarity with the analogous intertidal sample SM-B regarding grain size fraction percentage (Figure 3), with a slightly higher mean size. Its carbonate content is slightly lower compared to all SM samples: ~ 86 % (Table 5). A dominant mineral is a biogenous and terrigenous calcite,

while biogenous aragonite and terrigenous quartz are less present (Table 6). Besides the main sediment-building minerals, bustamite, calcium manganese oxide, and carbon are also found in the MM bulk sample, while bustamite is found in the MM mud fraction. The Mn-rich phases indicate the anthropogenic impact on the sediments in the Šibenik Bay, caused by the industrial production of manganese ferroalloys in the former TEF plant (Electrode and Ferroalloy Plant), as shown by Huljek et al. (2021). These authors also showed that anthropogenic impact is confined to the surface sediment (up to 5 cm), and the number of manganese compounds in sediment decreases with sediment depth. TOC in MM is slightly higher (> 6 %) compared to SM sediment, however, all MM sediment characteristics are similar to results presented by Prohić and Juračić (1989). Additional confirmation of obtained results are low values of TM in exchangeable fraction (BCR 1) (Table 7) at SM, while at the MM these values are multi-folded, especially for Zn (over 44 times), while for Pb and Cu values were under detection limit at SM location.

Concentrations of dissolved Zn and Cd in seawater samples were higher at SM compared to MM, while Cu showed higher values at the MM site (Table 4). Concentrations of dissolved Pb were almost identical at both locations, while total Pb was 25 % higher at the MM site, where Cd and Cu were predominantly in a dissolved state, 98 % and 83 % of total metal, respectively, and quite similar to SM site. However, only 45 % of Zn and 39 % of Pb were dissolved at the MM site, suggesting higher amounts of suspended matter in the water columns of MM compared to the SM site.

Two studied sites showed different anthropogenic influences, which is partly reflected in the sediment composition and thus in the chemical analysis. The MM sediment composition reflects the long-term existence of a closed ferroalloy plant in the vicinity of the site (Šibenik Bay). This can be seen in the additional mineral phases, total chemical analysis with *AR* (Huljek et al., 2021), and the first step of the BCR procedure when compared to the sediment of the SM cove. Concerning the exchangeable phase, the information from the first step of the BCR is important. At both sampling locations, the relation among the elements between seawater (Table 4) and BCR1 (Table 7) can be described: as the higher the metal concentration in seawater, the lower the BCR1 value, and vice versa.

5. Conclusion

Two study sites, selected for their different anthropogenic influence and similar geological and sedimentological background, revealed a difference in plastic particle abundance by plastic type and chemical composition of adsorbed elements on marine plastic litter. The number of MP particles are predominantly defined by local wave climate due to which SM cove had a higher number of microplastic particle per gram of beached debris in comparison with the MM cove of 9 times when comparing particles > 4 mm, or 2 times considering the bulk material. Different plastic types are defined at two locations; LDPE dominated at SM site, while similar amounts of PS and PP are present at MM site. 8 % of all analyzed plastic particles have been degraded beyond possibility of identification by FTIR-ATR.

Marine plastic particles were undoubtedly the medium for transport of toxic metals and the source of TM. The adsorption affinity for specific TM depends not only on the type of plastic but also on its size. The amounts of elements in the seawater and adsorbed on MP indicate that the environmental conditions were reflected on the plastic particles and as such were even predominantly noticeable on smaller particles. Considering the types of plastic and their affinity for certain elements, PS shows the highest affinity for all analyzed elements, particularly for Zn. Moreover, the smallest fraction of PS (0.250 – 1 mm) had twice the affinity for Zn, Cd, and Pb and more than 1.5 times the affinity for Cu, compared to PS particles > 4 mm. This dependence was also observed on plastic bulk material, with even greater differences, namely more than 5 times for Zn and Pb and 4 times for Cu. It can be suggested that the plastics affinity for metals followed order: PS > PP > LDPE. Moreover, Zn showed the strongest affinity for bulk plastics, followed by Cu and Pb in similar concentrations, while Cd showed the lowest adsorbed amounts.

Based on the average metal concentration on all analyzed samples defined as LDPE, Zn could be identified as an element with more than 6-fold higher affinity for LDPE than other elements (Cd, Pb, and Cu). In the samples defined as PP, the highest affinity is observed for Pb, which concentrations were even 30 times higher compared to LDPE, followed by Zn and Cu, which had more than 9- and 6-fold higher affinity than in LDPE, respectively, while Cd showed similar amounts on PP and LDPE. In the PS samples, the affinity of all elements is higher compared to LDPE and PP, as follows: Zn > Pb ≈ Cu > Cd.

Acknowledgement

This work has been fully supported by Croatian Science Foundation under the project IP-2019-04-5832.

The authors would like to thank Željka Fiket, PhD, from Division for Marine and Environmental Research, Ruđer Bošković Institute, for HR-ICP-MS analyses.

References

AGI, Australian Government Initiative. 2019. Toxicant default guideline values for sediment quality. Available online: https://www. waterquality.gov.au/anz-guidelines/guideline-values/default/sediment-quality-toxicants.

Andrady, A.L., 2011. Microplastics in the marine environment. Mar. Pollut. Bull. 62, 1596-1605. DOI: 10.1016/J.MARPOLBUL.2011.05.030

Ashton, K., Holmes, L., Turner, A., 2010. Association of metals with plastic production pellets in the marine environment. Mar. Pollut. Bull. 60, 2050-2055. DOI: 10.1016/J.MARPOLBUL.2010.07.014

Bakke, T., Källqvist, T., Ruus, A., Breedveld, G.D., Hylland, K., 2010. Development of sediment quality criteria in Norway. J. Soils Sediments, 10, 172-178. https://doi.org/10.1007/s11368-009-0173-y

Bard, A.J., Faulkner, L.R., 2001. Electrochemical Methods: Fundamentals and Applications, 2nd Edition, Wiley. URL https://www.wiley.com/en-be/Electrochemical+Methods:+Fundamentals+and+Applications,+2nd+Edition-p-9780471043720

Barus, B.S., Chen, K., Cai, M., Li, R., Chen, H., Li, C., Wang, J., Cheng, S.Y., 2021. Heavy Metal Adsorption and Release on Polystyrene Particles at Various Salinities. Front. Mar. Sci. 8, 596. DOI: 10.3389/FMARS.2021.671802/BIBTEX

Bergmann, M., Wirzberger, V., Krumpen, T., Lorenz, C., Primpke, S., Tekman, M.B., Gerdts, G., 2017. High Quantities of Microplastic in Arctic Deep-Sea Sediments from the HAUSGARTEN Observatory. Environ. Sci. Technol. 51, 11000-11010. DOI: 10.1021/ACS.EST.7B03331/SUPPL_FILE/ES7B03331_SI_001.PDF

Bonhomme, S., Cuer, A., Delort, A.M., Lemaire, J., Sancelme, M., Scott, G., 2003. Environmental biodegradation of polyethylene. Polym. Degrad. Stab. 81, 441-452. DOI: 10.1016/S0141-3910(03)00129-0

Browne, M.A., Crump, P., Niven, S.J., Teuten, E., Tonkin, A., Galloway, T., Thompson, R., 2011. Accumulation of Microplastic on Shorelines Woldwide: Sources and Sinks. Environ. Sci. Technol. 45, 9175-9179. DOI: 10.1021/ES201811S

CHI, 2015. Croatia Small Chart portfolio Part 2. 1:100 000, Croatian Hydrographic Institute.

Courtene-Jones, W., Quinn, B., Gary, S.F., Mogg, A.O.M., Narayanaswamy, B.E., 2017. Microplastic pollution identified in deep-sea water and ingested by benthic invertebrates in the Rockall Trough, North Atlantic Ocean. Environ Pollut 231, 271-280. DOI: 10.1016/J.ENVPOL.2017.08.026

Cózar, A., Echevarría, F., González-Gordillo, J.I., Irigoien, X., Ubeda, B., Hernández-León, S., Alvaro, T.N., García-de-Lomas, J., Ruiz, A., Fernández-de-Puelles, M.L., Duarte, C.M., 2015. Plastic Accumulation in the Mediterranean Sea. PLOS ONE 10, e0121762. DOI: 10.1371/JOURNAL.PONE.0121762

Cózar, A., Echevarría, F., González-Gordillo, J.I., Irigoien, X., Úbeda, B., Hernández-León, S., Palma, Á.T., Navarro, S., García-de-Lomas, J., Ruiz, A., Fernández-de-Puelles, M.L., Duarte, C.M., 2014. Plastic debris in the open ocean. Proc Natl Acad Sci U S A 111, 10239-10244. DOI: 10.1073/PNAS.1314705111/-/DCSUPPLEMENTAL/PNAS.1314705111.SAPP.PDF

Cuculić, V., Cukrov, N., Kwokal, Ž., Mlakar, M., 2009. Natural and anthropogenic sources of Hg, Cd, Pb, Cu and Zn in seawater and sediment of Mljet National Park, Croatia. Estuar. Coast. Shelf. Sci. 81, 311-320. DOI: 10.1016/J.ECSS.2008.11.006

Cuculić, V., Fajković, H., Kwokal, Ž., Matekalo, R., 2021. Trace metals load on beached microplastics in the anthropogenically influenced estuarine environment - Croatian middle Adriatic. EGU General Assembly 2021. DOI: 10.5194/EGUSPHERE-EGU21-1171

Davis, J.C., 2002. Statistics and Data Analysis in Geology, 3rd Edition, Wiley. John Wiley & Sons. URL https://www.wiley.com/en-gb/Statistics+and+Data+Analysis+in+Geology,+3rd+Edition-p-9780471172758.

EN ISO 10693:2014 - Soil quality - Determination of carbonate content - Volumetric method (ISO [WWW Document], n.d. URL https://standards.iteh.ai/catalog/standards/cen/822b8ccb-584d-4cd9-8f31-8cdf923f1406/en-iso-10693-2014.

Esiukova, E., 2017. Plastic pollution on the Baltic beaches of Kaliningrad region, Russia. Mar. Pollut. Bull. 114, 1072-1080. DOI: 10.1016/J.MARPOLBUL.2016.10.001

European Union. Directive 2008/56/EC EU Parliament and Council on the Establishing a Framework for Community Action in the Field of Marine Environmental Policy (Marine Strategy Framework Directive), 2008 O.J. L 164/19. - EN - EUR-Lex [WWW Document], n.d. URL https://eur-lex.europa.eu/legal-content/EN/TXT/?uri=celex%3A32008L0056%20A%20ovo%20je%20referenca:%20Directive%202008/56/EC%20EU%20Parliament%20and%20Council%20on%20the%20Establishing%20a%20Framework%20for%20Community%20Action%20in%20the%20Field%20of%20Marine%20Environmental%20Policy%20(Marine%20Strategy%20Framework%20Directive),%202008%20O.J.%20L%20164/19.

European Union. Directive 2000/60/EC of the European Parliament and of the Council of 23 October 2000 Establishing a Framework for Community Action in the Field of Water Policy. Available online: https://eur-lex.europa.eu/legal-content/EN/TXT/HTML/?uri=CELEX:32000L0060&from=EN

European Union. Directive 2010/75/EU of the European Parliament and of the Council of 24 November 2010 on Industrial Emissions (Integrated Pollution Prevention and Control). Available online: https://eur-lex.europa.eu/LexUriServ/LexUriServ.do?uri=OJ:L:2010:334:0017:0119:en:PDF

Fajković, H., Cukrov, N., Kwokal, Ž., Pikelj, K., Huljek, L., Kostanjšek, I., Cuculić, V., 2021. Correlation of microplastic type and metal association: Croatian coast case study (Žirje Island). EGU21. DOI: 10.5194/EGUSPHERE-EGU21-1022

Fernández Alborés, A.; Pérez Cid, B.; Fernández Gómez, E.; Falqué López, E. Comparison between sequential extraction procedures and single extractions for metal partitioning in sewage sludge samples. Analyst 2000, 125, 1353–1357. DOI: 10.1039/B001983F

Fiket, Ž., Mikac, N., Kniewald, G., 2017. Mass Fractions of Forty-Six Major and Trace Elements, Including Rare Earth Elements, in Sediment and Soil Reference Materials Used in Environmental Studies. Geostand. Geoanalytical Res. 41, 123-135. DOI: 10.1111/GGR.12129

Filgueiras, A. V., Lavilla, I., Bendicho, C. 2002. Chemical sequential extraction for metal partitioning in environmental solid samples. Journal of Environmental Monitoring, 4(6), 823–857. https://doi.org/10.1039/B207574C

Folk, R.L., 1954. The Distinction between Grain Size and Mineral Composition in Sedimentary-Rock Nomenclature. J. Geol. 62, 344-359. DOI: 10.1086/626171 62, 344-359. DOI: 10.1086/626171

Folk, R.L., Ward, W.C., Folk, R.L., Ward, W.C., 1957. Brazos River bar [Texas]; a study in the significance of grain size parameters. JSedR 27, 3-26. DOI: 10.1306/74D70646-2B21-11D7-8648000102C1865D

Frias, J.P.G.L., Nash, R., 2019. Microplastics: Finding a consensus on the definition. Mar. Pollut. Bull. 138, 145-147. DOI: 10.1016/J.MARPOLBUL.2018.11.022

Gao, L., Fu, D., Zhao, J., Wu, W., Wang, Z., Su, Y., Peng, L., 2021. Microplastics aged in various environmental media exhibited strong sorption to heavy metals in seawater. Mar. Pollut. Bull. 169. DOI: 10.1016/J.MARPOLBUL.2021.112480

Graca, B., Bełdowska, M., Wrzesień, P., Zgrundo, A., 2014. Styrofoam debris as a potential carrier of mercury within ecosystems. Environ. Sci. Pollut. Res. 21, 2263-2271. DOI: 10.1007/S11356-013-2153-4/FIGURES/6

Halamić, J., Peh, Z., Bukovec, D., Miko, S., Galović, L., 2001. A Factor Model of the Relationship between Stream Sediment Geochemistry and Adjacent Drainage Basin Lithology, Medvednica Mt., Croatia. Geol.a Croat. 54, 37-51.

Hernández-Moreno, J.M.; Rodríguez-González, J.I.; Espino-Mesa, M. Evaluation of the BCR sequential extraction for trace elements in European reference volcanic soils. Eur. J. Soil Sci. 2007, 58, 419–430. DOI: 10.1111/j.1365-2389.2007.00892.x

Hessler, A.M., Fildani, A., 2019. Deep-sea fans: tapping into Earth's changing landscapes. J. Sediment. Res. 89, 1171-1179. DOI: 10.2110/JSR.2019.64

Hildebrandt, L., Nack, F.L., Zimmermann, T., Pröfrock, D., 2021. Microplastics as a Trojan horse for trace metals. J. Hazard. Mater. 2, 100035. DOI: 10.1016/J.HAZL.2021.100035

Holmes, L.A., Turner, A., Thompson, R.C., 2012. Adsorption of trace metals to plastic resin pellets in the marine environment. Environ. Pollut. 160, 42-48. DOI: 10.1016/J.ENVPOL.2011.08.052

Horowitz, A.J., 1997. Some thoughts on problems associated with various sampling media used for environmental monitoring. Analyst 122, 1193-1200. DOI: 10.1039/A704604I

Huljek, L., Palinkaš, S.S., Fiket, Ž., Fajković, H., 2021. Environmental Aspects of Historical Ferromanganese Tailings in the Šibenik Bay, Croatia. Water 2021, Vol. 13, Page 3123 13, 3123. DOI: 10.3390/W13213123

Ioakeimidis, C., Zeri, C., Kaberi, H., Galatchi, M., Antoniadis, K., Streftaris, N., Galgani, F., Papathanassiou, E., Papatheodorou, G., 2014. A comparative study of marine litter on the seafloor of coastal areas in the Eastern Mediterranean and Black Seas. Mar. Pollut. Bull. 89, 296-304. DOI: 10.1016/J.MARPOLBUL.2014.09.044

Jung, M.R., Horgen, F.D., Orski, S. v., Rodriguez C., V., Beers, K.L., Balazs, G.H., Jones, T.T., Work, T.M., Brignac, K.C., Royer, S.J., Hyrenbach, K.D., Jensen, B.A., Lynch, J.M., 2018. Validation of ATR FT-IR to identify polymers of plastic marine debris, including those ingested by marine organisms. Mar. Pollut. Bull. 127, 704-716. DOI: 10.1016/J.MARPOLBUL.2017.12.061

Kane, I.A., Fildani, A., 2021. Anthropogenic pollution in deep-marine sedimentary systems—A geological perspective on the plastic problem. Geology 49, 607-608. DOI: 10.1130/FOCUS052021.1

Kaufman, L., Rousseeuw, P.J., 1990. Finding Groups in Data - Wiley Series on Probability and Mathematical Statistics Chapters 2 & 3.

Kowalski, N., Reichardt, A.M., Waniek, J.J., 2016. Sinking rates of microplastics and potential implications of their alteration by physical, biological, and chemical factors. Mar. Pollut. Bull.109, 310-319. DOI: 10.1016/J.MARPOLBUL.2016.05.064

Kwokal, Ž., Cuculić, V., 2016. Pre-production plastic pellets as a transport medium of mercury along the eastern Adriatic coast (Croatia), in: 41st CIESM Congress Proceedings. p. 221.

Kwokal, Ž., Štefanović, B., 2010. Floating marine litter without boundaries: a threat to the coves of Mljet Island (Croatia). Proceedings of the Symposium of Branimir Gusic Days - Mljet. pp. 349-362.

Kwokal, Ž., Štefanović, B., 2009. Floating marine litter, neglecting does not mean absence, in: Visković, L. (Ed.), 2. Adriatic Boat Show. Šibenik, pp. 3-10.

Lacombe, H., Gascard, J.C., Gonella, J., Béthoux, J.P., 1981. OCEANOLOGICA ACTA 1981-VOL. 4-Na 2 ~ ·Response of the Mediterranean to the water and energy fluxes Ocean-atmosphere interaction Mediterranean Sea Hydrology Seasonal variation lnterannual variation Interaction océan-

atmosphère Mer Méditerranée Hydrologie Variations saisonnières Variations inter-annuelles across its surface, on seasonal and interannual scales ABSTRACT RÉSUMÉ 4, 247-255.

Law, K.L., Morét-Ferguson, S., Maximenko, N.A., Proskurowski, G., Peacock, E.E., Hafner, J., Reddy, C.M., 2010. Plastic accumulation in the North Atlantic subtropical gyre. Science 329, 1185-1188. DOI: 10.1126/SCIENCE.1192321/SUPPL_FILE/LAW_SOM_REVISION_1.PDF

Lee, A., Mondon, J., Merenda, A., Dumée, L.F., Callahan, D.L., 2021. Surface adsorption of metallic species onto microplastics with long-term exposure to the natural marine environment. Sci. Total. Environ. 780. DOI: 10.1016/J.SCITOTENV.2021.146613

Lee, D.I., Cho, H.S., Jeong, S.B., 2006. Distribution characteristics of marine litter on the sea bed of the East China Sea and the South Sea of Korea. Estuar. Coast. Shelf Sci. 70, 187-194. DOI: 10.1016/J.ECSS.2006.06.003

Liubartseva, S., Coppini, G., Lecci, R., Creti, S., 2016. Regional approach to modeling the transport of floating plastic debris in the Adriatic Sea. Mar. Pollut. Bull. 103, 115-127. DOI: 10.1016/J.MARPOLBUL.2015.12.031

Mamužić, P., 1982. Basic geological map of the SFRY 1:100 000, Šibenik sheet K33-8. Basic geological map of the SFRY 1:100 000, Šibenik sheet K33-8.

Marinčić, S., Magaš, N., Blašković, I., 1971. Basic geological map of the SFRY 1:100 000, Primošten sheet K33-20. Institut za geološka istraživanja, Zagreb; Savezni geološki Institut Beograd.

Maršić-Lučić, J., Lušić, J., Tutman, P., Bojanić Varezić, D., Šiljić, J., Pribudić, J., 2018. Levels of trace metals on microplastic particles in beach sediments of the island of Vis, Adriatic Sea, Croatia. Mar. Pollut. Bull. 137, 231-236. DOI: 10.1016/J.MARPOLBUL.2018.10.027

Martin, J., Lusher, A., Thompson, R.C., Morley, A., 2017. The Deposition and Accumulation of Microplastics in Marine Sediments and Bottom Water from the Irish Continental Shelf. Sci. Rep. 2017 7:1 7, 1-9. DOI: 10.1038/s41598-017-11079-2

Massos, A., Turner, A., 2017. Cadmium, lead and bromine in beached microplastics. Environ. Pollut. 227, 139-145. DOI: 10.1016/J.ENVPOL.2017.04.034

MICROMERITICS, 2002. SediGraph 5100 Particle size analysis system operator' manual.

Mistri, M., Infantini, V., Scoponi, M., Granata, T., Moruzzi, L., Massara, F., de Donati, M., Munari, C., 2017. Small plastic debris in sediments from the Central Adriatic Sea: Types, occurrence and distribution. Mar. Pollut. Bull. 124, 435-440. DOI: 10.1016/J.MARPOLBUL.2017.07.063

Munier, B., Bendell, L.I., 2018. Macro and micro plastics sorb and desorb metals and act as a point source of trace metals to coastal ecosystems. PLOS ONE 13, e0191759. DOI: 10.1371/JOURNAL.PONE.0191759

Naji, A., Esmaili, Z., Khan, F.R., 2017. Plastic debris and microplastics along the beaches of the Strait of Hormuz, Persian Gulf. Mar. Pollut. Bull. 114, 1057-1062. DOI: 10.1016/J.MARPOLBUL.2016.11.032

Nakashima, E., Isobe, A., Kako, S., Itai, T., Takahashi, S., 2012. Quantification of toxic metals derived from macroplastic litter on Ookushi Beach, Japan. Environ. Sci. Technol. 46, 10099-10105. DOI: 10.1021/ES301362G

Neff, J.M., 2002. Cadmium in the Ocean. Bioaccumulation in Marine Organisms 89-102. DOI: 10.1016/B978-008043716-3/50006-3

Pasquini, G., Ronchi, F., Strafella, P., Scarcella, G., Fortibuoni, T., 2016. Seabed litter composition, distribution and sources in the Northern and Central Adriatic Sea (Mediterranean). Waste Manage. 58, 41-51. DOI: 10.1016/J.WASMAN.2016.08.038

Pedrotti, M.L., Petit, S., Elineau, A., Bruzaud, S., Crebassa, J.C., Dumontet, B., Martí, E., Gorsky, G., Cózar, A., 2016. Changes in the Floating Plastic Pollution of the Mediterranean Sea in Relation to the Distance to Land. PLOS ONE 11, e0161581. DOI: 10.1371/JOURNAL.PONE.0161581

Peng, X., Chen, M., Chen, S., Dasgupta, S., Xu, H., Ta, K., Du, M., Li, J., Guo, Z., Bai, S., 2018. Microplastics contaminate the deepest part of the world's ocean. Geochem. Perspect. Lett. 9, 1-5. DOI: 10.7185/GEOCHEMLET.1829

Pikelj, K., 2010. Composition and origin of seabed sediments of the eastern part of the Adriatic Sea (in Croatian). Ph.D. Thesis, University of Zagreb, p. 239.

Pikelj, K., Jakšić, L., Aščić, Š., Juračić, M., 2016. Characterization of the fine-grained fraction in the surface sediment of the eastern Adriatic channel areas. Acta Adriat., 57/2 195-208.

Pikelj, K., Juračić, M., 2013. Eastern Adriatic Coast (EAC): Geomorphology and Coastal Vulnerability of a Karstic Coast. J. Coast. Res. 29, 944-957. DOI: 10.2112/JCOASTRES-D-12-00136.1

Poulain, P.-M., Cushman-Roisin, B. (2001): Circulation. In: B. Cushman-Roisin, M. Gačić, P.-M. Poulain, A. Artegiani (Eds): Physical Oceanography of the Adriatic Sea: Past, Present and Future. Kluwer Academic Publishers, Dordrecht, 67-109.

Prohić, E., Juračić, M., 1989. Heavy metals in sediments - problems concerning determination of the anthropogenic influence. Study in the Krka River estuary, eastern Adriatic coast, Yugoslavia. Environ. Geol. 13, 145-151. DOI: 10.1007/BF01664699

Pueyo, M., Mateu, J., Rigol, A., Vidal, M., López-Sánchez, J.F., Rauret, G., 2008. Use of the modified BCR three-step sequential extraction procedure for the study of trace element dynamics in contaminated soils. Environ. Pollut. 152, 330-341. DOI: 10.1016/J.ENVPOL.2007.06.020

Puhr, K., Pikelj, K., 2012. The effect of *in situ* shading on a *Posidonia oceanica* meadow situated within a fish farm induced moderately nutrient enriched environment. Mar. Pollut. Bull. 64, 1537-1548. DOI: 10.1016/J.MARPOLBUL.2012.05.022

Radix, P., Léonard, M., Papantoniou, C., Roman, G., Saouter, E., Gallotti-Schmitt, S., Thiébaud, H., Vasseur, P., 2000. Comparison of four chronic toxicity tests using algae, bacteria, and invertebrates assessed with sixteen chemicals. Ecotoxicol. Environ. Saf. 47, 186-194. DOI: 10.1006/EESA.2000.1966

Rauret, G., López-Sánchez, J.F., Sahuquillo, A., Rubio, R., Davidson, C., Ure, A., Quevauviller, P., 1999. Improvement of the BCR three step sequential extraction procedure prior to the certification of new sediment and soil reference materials. J. Environ. Monit. 1, 57-61. DOI: 10.1039/A807854H

Reimann, C., Filzmoser, P., Garrett, R.G., 2005. Background and threshold: critical comparison of methods of determination. Sci. Total Environ. 346, 1-16. DOI: 10.1016/J.SCITOTENV.2004.11.023

Rochman, C.M., 2013. Plastics and Priority Pollutants: A Multiple Stressor in Aquatic Habitats. Environ. Sci. Technol. 47, 2439-2440. DOI: 10.1021/ES400748B

Rochman, C.M., Hentschel, B.T., The, S.J., 2014. Long-Term Sorption of Metals Is Similar among Plastic Types: Implications for Plastic Debris in Aquatic Environments. PLOS ONE 9, e85433. DOI: 10.1371/JOURNAL.PONE.0085433

Sagawa, N., Kawaai, K., Hinata, H., 2018. Abundance and size of microplastics in a coastal sea: Comparison among bottom sediment, beach sediment, and surface water. Mar. Pollut. Bull. 133, 532-542. DOI: 10.1016/j.marpolbul.2018.05.036

Schmid, C., Cozzarini, L., Zambello, E., 2021. A critical review on marine litter in the Adriatic Sea: Focus on plastic pollution. Environ. Pollut. 273. DOI: 10.1016/J.ENVPOL.2021.116430

StatSoft, Inc., 2001. STATISTICA Data Analysis Software System.

Ta, A.T., Babel, S., 2020. Microplastics pollution with heavy metals in the aquaculture zone of the Chao Phraya River Estuary, Thailand. Mar. Pollut. Bull. 161, 111747. DOI: 10.1016/J.MARPOLBUL.2020.111747

Tziourrou, P., Megalovasilis, P., Tsounia, M., Karapanagioti, H.K., 2019. Characteristics of microplastics on two beaches affected by different land uses in Salamina Island in Saronikos Gulf, east Mediterranean. Mar. Pollut. Bull. 149. DOI: 10.1016/J.MARPOLBUL.2019.110531

Vdović, N., Juračić, M., 1993. Sedimentological and Surface Characteristics of the Northern and Central Adriatic Sediments. Geol. Croat. 46, 157-163.

Vlachogianni, T., Fortibuoni, T., Ronchi, F., Zeri, C., Mazziotti, C., Tutman, P., Varezić, D.B., Palatinus, A., Trdan, Š., Peterlin, M., Mandić, M., Markovic, O., Prvan, M., Kaberi, H., Prevenios, M., Kolitari, J., Kroqi, G., Fusco, M., Kalampokis, E., Scoullos, M., 2018. Marine litter on the beaches of the Adriatic and Ionian Seas: An assessment of their abundance, composition and sources. Mar. Pollut. Bull. 131, 745-756. DOI: 10.1016/J.MARPOLBUL.2018.05.006

Wang, J., Peng, J., Tan, Z., Gao, Y., Zhan, Z., Chen, Q., Cai, L., 2017. Microplastics in the surface sediments from the Beijiang River littoral zone: Composition, abundance, surface textures and interaction with heavy metals. Chemosphere 171, 248-258. DOI: 10.1016/J.CHEMOSPHERE.2016.12.074

Xie, M., Huang, J.L., Lin, Z., Chen, R., Tan, Q.G., 2021. Field to laboratory comparison of metal accumulation on aged microplastics in coastal waters. Sci. Total Environ. 797, 149108. DOI: 10.1016/J.SCITOTENV.2021.149108

Zambianchi, E., Trani, M., Falco, P., 2017. Lagrangian transport of marine litter in the Mediterranean Sea. Front. Environ. Sci 5:5. DOI: 10.3389/FENVS.2017.00005/BIBTEX

Zeri, C., Adamopoulou, A., Bojanić Varezić, D., Fortibuoni, T., Kovač Viršek, M., Kržan, A., Mandić, M., Mazziotti, C., Palatinuš, A., Peterlin, M., Prvan, M., Ronchi, F., Šiljić, J., Tutman, P., Vlachogianni, T., 2018. Floating plastics in Adriatic waters (Mediterranean Sea): From the macro- to the micro-scale. Mar. Pollut. Bull. 136, 341-350. DOI: 10.1016/J.MARPOLBUL.2018.09.016

Figure captions

Fig. 1. Sampling locations and geological setting of the wider area; (simplified after Mamužić, 1982; Marinčić et al., 1971). Legend: 1 - Quaternary deposits and terra rossa; 2 - Eocene flysch; 3 - Eocene limestones; 4 - Palaeocene-Eocene limestones; 5 - Cretaceous limestones (Senonian); 6 - Cretaceous limestones and dolomites (Albian-Cenomanian); 7 - Cretaceous dolomites (Albian-Cenomanian); 8 - all boundaries; 9 - all faults; 10 - sampling locations; 11 - Šibenik urban zone; 12 - dominant Jugo/Scirocco wave direction.

Fig. 2. Representative FTIR spectra of extracted microplastics.

Fig. 3. Classification of SM and MM sediments based on the gravel/sand/mud ratios (Folk, 1954).

Fig. 4. Scatterplots with Boxplots for elements in collected plastic particles from sampling locations SM (left) and MM (right).

Fig. 5. Dendrogram (tree diagram – single linkage, Euclidean distances) for sampling locations SM (a) and MM (b).

Table 1. Number (#) of microplastic particles (MP).

Sample	Fraction size (mm)	# PS	# PP	# HDPE	# LDPE	# of n.d.*	Total	# MP/g D** per fraction
SM	> 4	2	15	0	48	6	71	
	# MP/ g D**	0.06	0.5	0	1.5	0.2		2.26
MM	> 4	2	2	2	0	0	6	0.25
	2-4	4	5	0	2	1	12	0.45
	1-2	4	0	0	0	1	5	0.23
	0.25-1	0	2	0	0	0	2	0.19
	# MP/ g D**	0.13	0.12	0.03	0.03	0.03		∑ 1.12

* n.d. - plastic type could not be determined
** D - debris

Table 2. Mass fractions of adsorbed TM (mg/kg) on the surface of defined plastic particles > 4 mm from SM site. c.i. - 95 % confidence interval.

Sample	Zn	c.i.	Cd	c.i.	Pb	c.i.	Cu	c.i.
LDPE_a	5.715	0.195	0.004	0.001	0.062	0.015	0.049	0.005
LDPE_b	3.639	0.273	2.825	0.159	1.506	0.030	0.191	0.017
LDPE_c	1.158	0.049	0.024	0.001	0.482	0.045	0.691	0.089
LDPE_d	4.796	0.192	0.023	0.005	0.290	0.049	1.476	0.150
LDPE_e	2.776	0.459	0.022	0.001	0.421	0.021	0.229	0.024
LDPE_f	2.717	0.062	0.112	0.011	0.534	0.053	0.662	0.077
PP_a	10.884	0.949	0.036	0.003	63.904	3.063	0.293	0.024
PP_b	1.759	0.001	1.115	0.135	10.889	0.835	0.318	0.001
PP_c	3.036	0.260	0.952	0.041	1.171	0.049	0.225	0.012
PP_d	6.271	0.249	0.438	0.019	7.506	0.486	16.593	1.682
PP_e	0.950	0.116	0.015	0.001	0.347	0.026	0.204	0.011
PS_a	71.533	4.871	0.084	0.014	10.926	0.567	9.783	0.726
N.D._a	1.823	0.062	0.021	0.001	0.200	0.023	0.063	0.005
N.D._b	0.670	0.006	0.005	0.000	0.136	0.014	0.227	0.013
N.D._c	1.947	0.067	0.328	0.011	0.913	0.021	0.289	0.001
$\bar{x}$	7.978	0.521	0.400	0.027	6.619	0.353	2.086	0.189

$\bar{x}$ - Arithmetic mean

Table 3. Mass fractions of adsorbed TM (mg/kg) on the surface of fractionated plastic particles defined as polystyrene (PS) and as mixed particles (Bulk) from MM site. c.i. - 95 % confidence interval.

Sample	Fraction size (mm)	Zn	c.i.	Cd	c.i.	Pb	c.i.	Cu	c.i.
PS	> 4	75.694	5.781	0.178	0.008	15.626	1.190	20.685	0.590
	2 - 4	50.060	1.619	0.134	0.002	11.121	0.628	13.018	0.199
	1 - 2	69.531	5.891	0.181	0.019	16.217	0.995	16.707	0.567
	0.250 - 1	146.537	10.767	0.352	0.026	34.056	3.567	32.894	3.202
	$\bar{x}$	85.456	6.014	0.211	0.013	19.255	1.595	20.826	1.140
Bulk	> 4	8.391	0.569	0.222	0.015	2.199	0.107	3.846	0.198
	2 - 4	5.942	0.486	0.016	0.001	1.145	0.097	1.738	0.145
	1 - 2	12.603	0.589	0.022	0.021	3.744	0.264	2.779	0.080
	0.250 - 1	49.249	1.640	0.172	0.001	13.031	1.122	15.476	0.141
	$\bar{x}$	19.046	0.821	0.108	0.009	5.030	0.397	5.960	0.141

$\bar{x}$ - Arithmetic mean

Table 4. Trace metal concentrations in seawater (ng/L); dissolved metal - diss; total metal - tot; percentage of dissolved metal - diss. (%). c.i. - 95 % confidence interval.

Sample	Zn	c.i.	Cd	c.i.	Pb	c.i.	Cu	c.i.
SM-diss	2496	284	20.5	2.7	31.8	2.1	353	26
SM-tot	3481	347	20.7	0.6	62.3	3.8	428	49
SM diss. (%)	71.7		99.2		51.1		82.3	
MM-diss	855	114	9.4	1.4	31.6	2.3	839	60
MM-tot	1883	66	9.6	1.2	80.3	4.5	1006	33
MM diss. (%)	45.4		97.8		39.4		83.4	

Table 5. Carbonate component (%) in SM and MM samples.

Fraction size (mm)	SM-A	SM-B	SM-C	MM
		(%)		
1 - 2	97.62	99.05	99.36	82.53
0.5 - 1	97.20	98.11	98.78	71.33
0.25 - 0.5	95.56	97.90	98.03	56.25
0.125 - 0.25	91.82	94.26	90.34	52.55
0.063 - 0.125	83.95	72.98	74.29	47.27
< 0.063	78.31	61.66	55.5	68.7
BULK	97.59	96.83	94.52	86.2

Table 6. Mineral phases in sample SM-B and MM, in bulk and fraction < 0.063 mm.

	Mineral phases							
Sample	Calcite	Quartz	Aragonite	Bustamite	CMO*	Carbon	Halite	Mg-calcite
SM-B, bulk	x	x	x					x
SM-B, mud	x	x	x					
MM, bulk	x		x	x	x	x	x	
MM, mud	x	x	x	x				

*CMO - Calcium Manganese Oxide

Table 7. The weight fraction of analyzed elements in SM-B and MM bulk sample obtained by first step of BCR sequential analysis (BCR1) with SD.

Sample		Zn	Cd	Pb	Cu
		(mg/kg)			
SM-B	BCR 1	0.811 ± 2.41	0.09 ± 0.045	LoD*	LoD
MM	BCR 1	35.82 ± 0.55	0.14 ± 0.01	0.91 ± 0.05	1.59 ± 0.01

* LoD Under limit of detection

Table 8. Basic statistical parameters of leached elements from MP.

Location	Element	Valid N	Mean	Median	Minimum	Maximum	Range	Variance	Std. Dev.
SM	Zn	18	9.53	4.56	0.95	71.53	70.58	265.91	16.31
	Cd	18	0.39	0.14	0.00	2.83	2.82	0.47	0.69
	Pb	18	6.35	1.41	0.06	63.90	63.84	218.87	14.79
	Cu	18	2.21	0.68	0.05	16.59	16.54	18.27	4.27
MM	Zn	8	52.25	49.65	5.94	146.54	140.60	2198.86	46.89
	Cd	8	0.16	0.17	0.02	0.35	0.34	0.01	0.11
	Pb	8	12.14	12.08	1.14	34.06	32.91	114.45	10.70
	Cu	8	13.39	14.25	1.74	32.89	31.16	112.65	10.61

Table 9. Correlation matrix between the elements adsorbed on plastic particles.

	SM location				MM location				
	Zn	Cd	Pb	Cu		Zn	Cd	Pb	Cu
Zn	1				Zn	1			
Cd	-0.12	1			Cd	**0.66**	1		
Pb	0.19	-0.09	1		Pb	**1**	**0.69**	1	
Cu	**0.49**	-0.06	0.05	1	Cu	**0.99**	**0.63**	**0.98**	1

Figure 1

Click here to access/download;Figure(s);Fig. 1.jpg

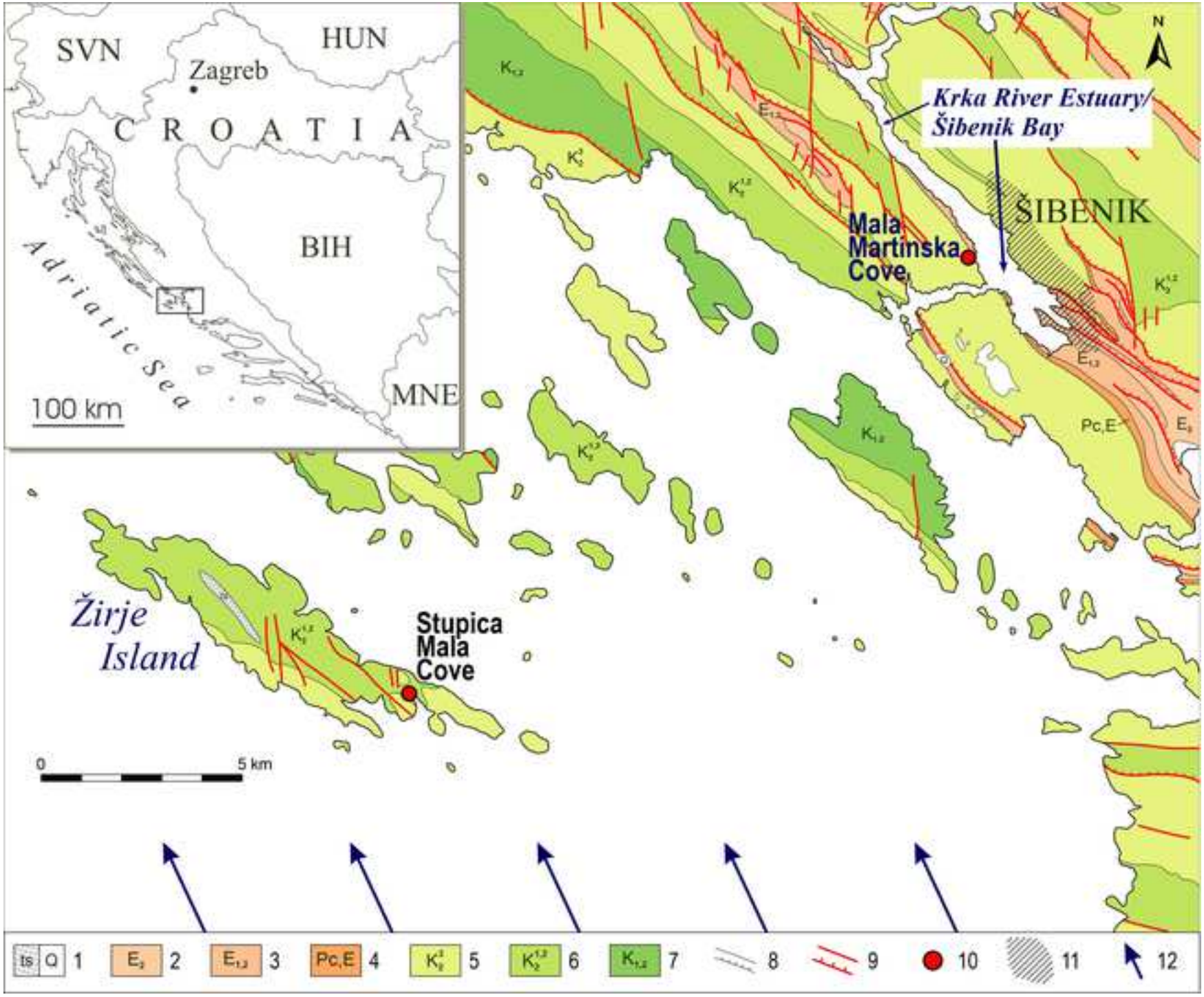

Figure 2

Click here to access/download;Figure(s);Fig. 2.jpg

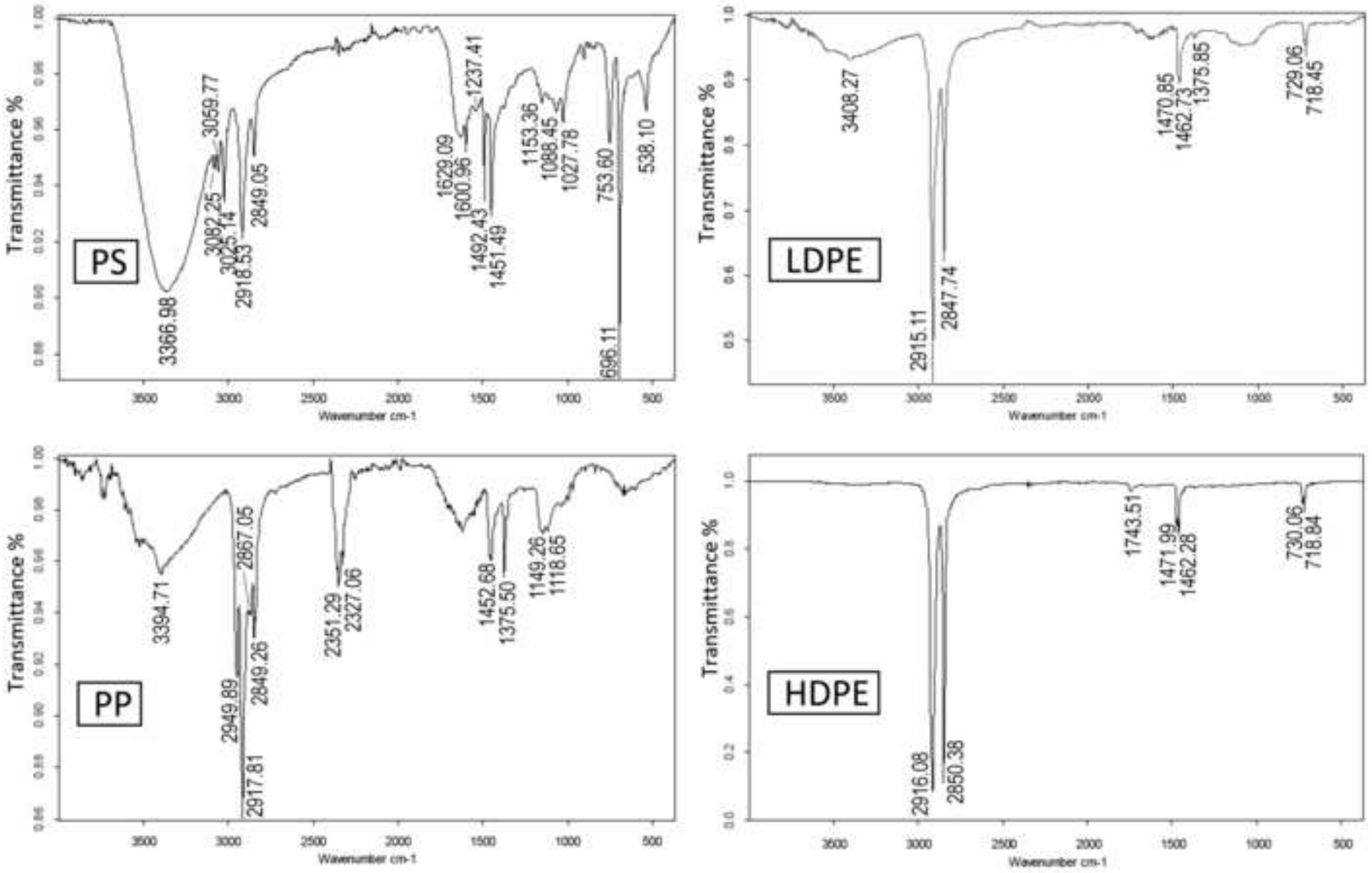

Figure 3

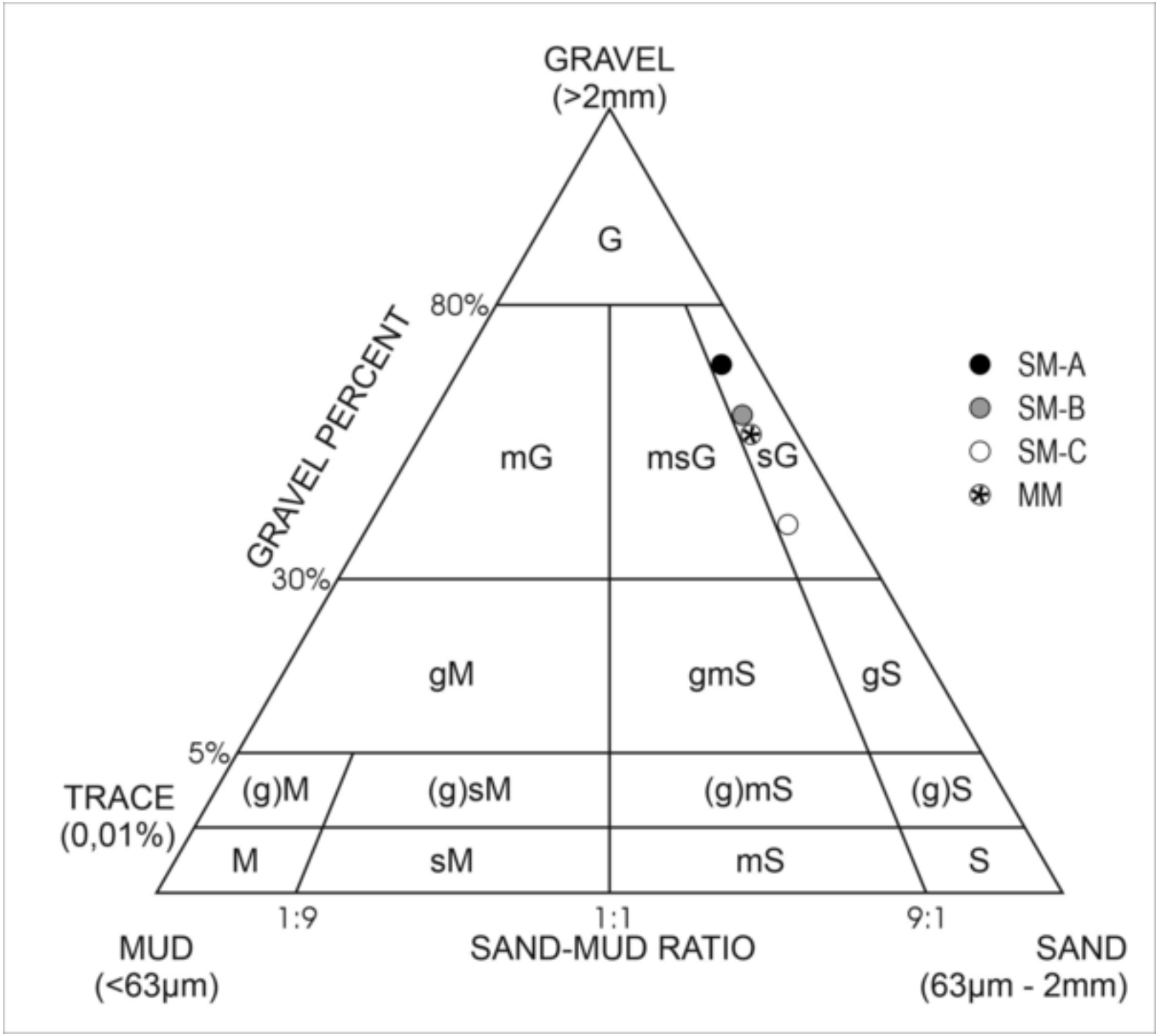

Figure 4

Click here to access/download;Figure(s);Fig. 4.jpg

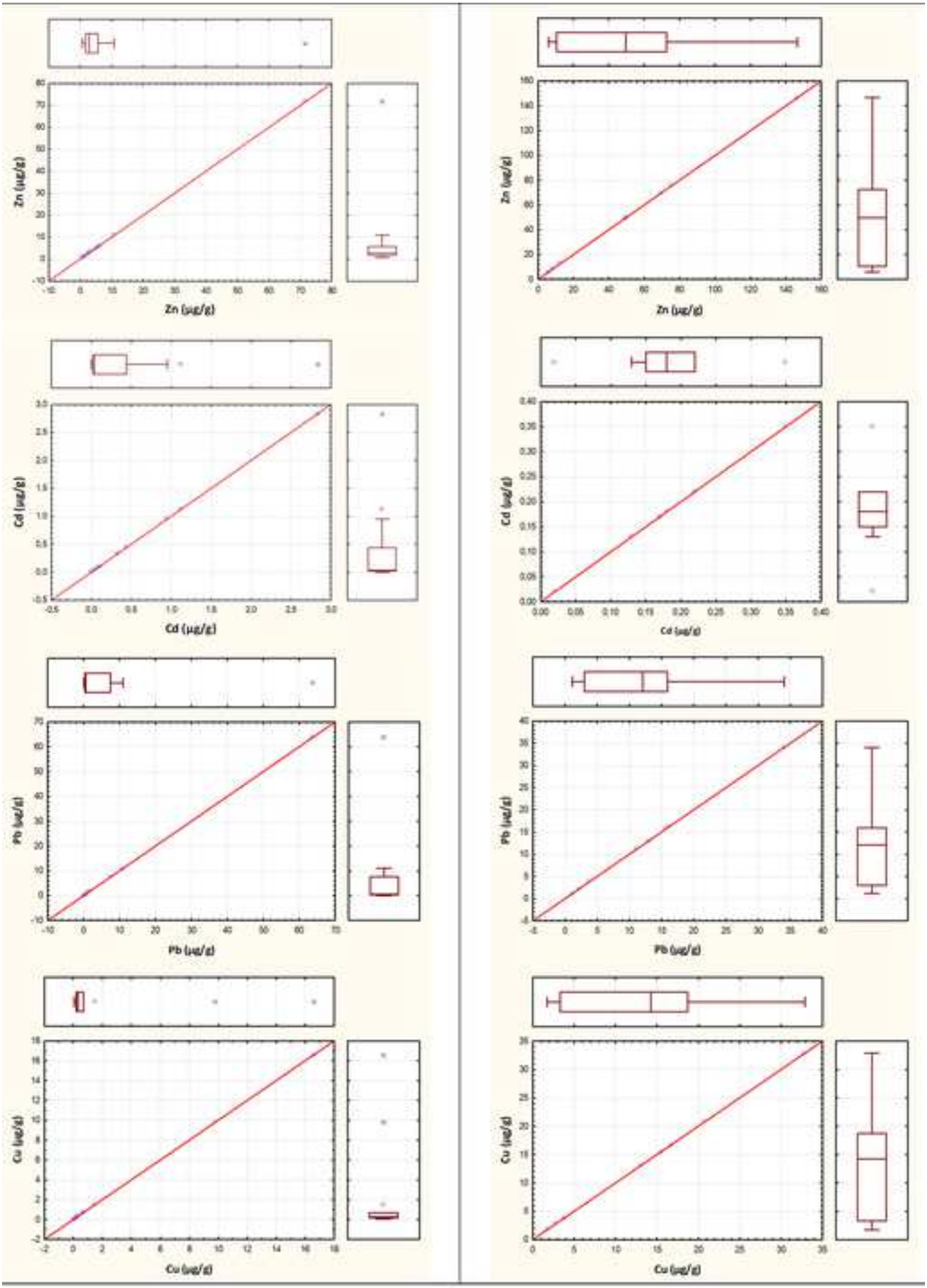

Figure 5

Click here to access/download;Figure(s);Fig. 5.JPG

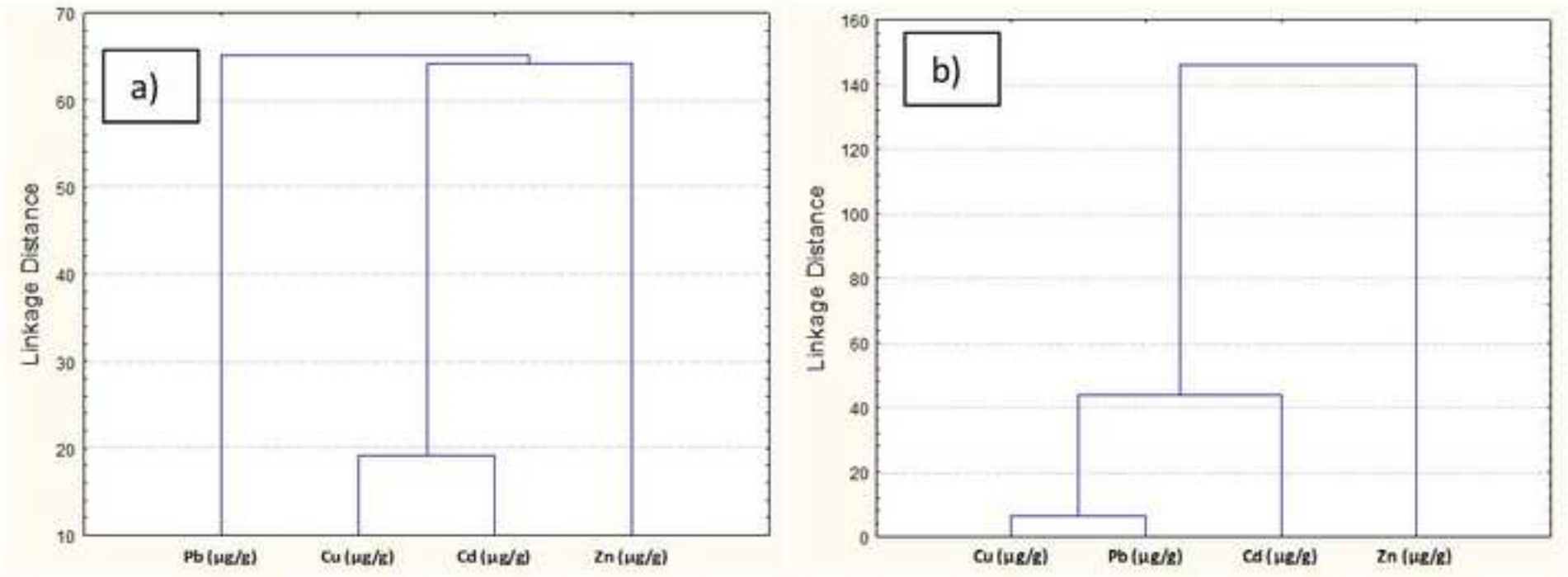

Declaration of interests

☒The authors declare that they have no known competing financial interests or personal relationships that could have appeared to influence the work reported in this paper.

☐The authors declare the following financial interests/personal relationships which may be considered as potential competing interests: